AD-A046 246 STATE UNIV OF NEW YORK AT STONY BROOK DEPT OF MATERIA--ETC F/G 11/6
PROPERTIES OF MATERIALS QUENCHED FROM THE LIQUID STATE.(U)
SEP 77 H HERMAN DA-AROD-31-124-70-G32

UNCLASSIFIED ARO-8571.11-MC NL

| OF |
ADA
046246

END
DATE
FILMED
12-77
DDC

ARO 8571.11-MC

12 pp.

PROPERTIES OF MATERIALS QUENCHED FROM THE LIQUID STATE.

FINAL REPORT.
1 Feb 70 - 30 Jun 76

Herbert Herman
Professor

1 September 1, 1977

36p.

U.S. ARMY RESEARCH OFFICE

DA-AROD-31-124-70-G32,
72-G70; 73-G169, and
DAHC04-75-G-0199 for the
Period 1 February 1970 - 30 June 1976

DEPARTMENT OF MATERIALS SCIENCE
STATE UNIVERSITY OF NEW YORK
STONY BROOK, N.Y. 11794

ARO 8571.11-MC

401 074

SECURITY CLASSIFICATION OF THIS PAGE *(When Data Entered)*

REPORT DOCUMENTATION PAGE

READ INSTRUCTIONS BEFORE COMPLETING FORM

1. REPORT NUMBER: Final Report	2. GOVT ACCESSION NO.
3. RECIPIENT'S CATALOG NUMBER	
4. TITLE *(and Subtitle)*: PROPERTIES OF MATERIALS QUENCHED FROM THE LIQUID STATE	5. TYPE OF REPORT & PERIOD COVERED: Final Report, 1 Feb. 1970 - 30 June 1976
	6. PERFORMING ORG. REPORT NUMBER
7. AUTHOR(s): Prof. Herbert Herman	8. CONTRACT OR GRANT NUMBER(s): DA-AROD-31-124-70-G32; 72-G70 Renew; 73-G169; DAHC04-75-G-0199
9. PERFORMING ORGANIZATION NAME AND ADDRESS: Department of Materials Science ✓ State University of New York Stony Brook, N.Y. 11794	10. PROGRAM ELEMENT, PROJECT, TASK AREA & WORK UNIT NUMBERS
11. CONTROLLING OFFICE NAME AND ADDRESS: U.S. Army Research Office Post Office Box 12211 Research Triangle Park, NC 27709	12. REPORT DATE: 1 Sept. 1977
	13. NUMBER OF PAGES: 29
14. MONITORING AGENCY NAME & ADDRESS *(if different from Controlling Office)*	15. SECURITY CLASS. *(of this report)*: Unclassified
	15a. DECLASSIFICATION/DOWNGRADING SCHEDULE: NA

16. DISTRIBUTION STATEMENT *(of this Report)*

Approved for public release; distribution unlimited.

17. DISTRIBUTION STATEMENT *(of the abstract entered in Block 20, if different from Report)*

NA

18. SUPPLEMENTARY NOTES

The findings in this report are not to be construed as an official Department of the Army position, unless so designated by other authorized documents.

19. KEY WORDS *(Continue on reverse side if necessary and identify by block number)*

Liquid quenching, splat cooling, laser melting, plasma spraying, spinodal decomposition, small-angle x-ray scattering, small-angle neutron scattering, rapid solidification.

20. ABSTRACT *(Continue on reverse side if necessary and identify by block number)*

Metal alloys and refractory oxides have been quenched (splat cooled) from the liquid state at ultra-high rates using a wide range of techniques. The alloys have been quenched by the standard shock-tube method, while oxides were quenched using laser methods or with plasma spraying. The rapid quench permits access into metastable regions of the phase diagram, thus yield ultra-high supersaturation. The earliest regime of precipitation reactions are able to be detected, and, thus, a linear spinodal process has →over

DD FORM JAN 73 1473 EDITION OF 1 NOV 65 IS OBSOLETE

20: (Continued)

been determined in several alloys. Liquid quenching is useful for studies of phase transformations, since the system can be obtained in highly metastable states. Small-angle x-ray and neutron scattering and transmission electron microscopy were used in this study.

TABLE OF CONTENTS

Properties of Materials Quenched From The Liquid State

		Page
I.	INTRODUCTION	1
II.	LQ DEVICES	2
	Shock Tube Method	2
	Torsion Catapult	2
	LQ of Laser-Melted Oxides	3
III.	REVIEWS OF ALLOY SYSTEMS STUDIED IN THIS PROGRAM	5
	Al-7 Zn	5
	Al-22 Zn	5
	Al-28 Zn	8
	Al-Ag	9
	Al-Si	11
	Ag-Ge	13
	Au-Ge	13
IV.	OXIDES WHICH HAVE BEEN STUDIED	13
	A. Laser Hammer-and-Anvil	14
	B. Laser LQ (Gun Blast)	15
	1. Unary Systems	15
	2. Binary Systems	15
	C. Theoretical Calculations	16
	D. Miscibility Gaps in Oxides	16
V.	PLASMA SPRAYING OF OXIDES	17
	A. Introduction	17
	B. Sample Preparation	17
	C. Characterization of Coatings	19
	Results and Discussion	19
VI.	CONCLUSIONS	25
	REFERENCES	27
VII.	PUBLICATIONS RESULTING FROM THIS ARO-SUPPORTED PROGRAM	28

FINAL REPORT

TO ARMY RESEARCH OFFICE

"Properties of Materials Quenched From the Liquid State"

H. Herman
Department of Materials Science
State University of New York
Stony Brook, N. Y. 11794

I. INTRODUCTION

This Army-supported research program on liquid-quenched (LQ) alloys and ceramics has evolved from the period of 1970 to 1976 from the fundamental to the applied. Initially, it was the goal of this study to examine in some detail the structures that develop on the annealing of LQ (splat cooled) alloys. The kinetics and resulting morphologies were subjected to careful examination rising x-rays and transmission electron microscopy (TEM). A central aspect of the program concentrated on small angle x-ray scattering (SAXS) from LQ aluminum-based alloys. The alloys of aluminum containing Ag and Zn are two systems which show spinodal decomposition behavior. In fact, linear spinodal behavior was observed to occur in this study when LQ samples were studied with SAXS.

Following the aluminum alloy studies, as well as other alloy system studies, oxides were examined. A number of LQ techniques were developed and explored, based mainly on laser melting and plasma spraying. The latter technique has in fact given rise to a new program - currently under support by ONR - on protective coatings. The spinodal work is currently culminating in a program partially funded by NATO (for international travel) and employing small-angle neutron scattering (SANS) at ILL-Grenoble, France, to study spinodal decomposition in the Pt-Au alloy system. (An additional point of interest relative to Au-Pt: In conjunction with workers at NRL - J. K. Hirvonen - and originating

from this ARO program, has emerged an interesting study using ion implantation to form highly metastable alloys. We have thus observed with TEM a spinodally decomposed amorphous surface in Au-implanted Pt. It is estimated that the "quench rate" in such a situation may be 10^{12}°C/sec!).

The U.S. Army Research Office program has thus enabled numerous closely related studies of the utilization - both scientific and applied - of LQ methods. New theoretical developments used to calculate the actual spinodal have evolved, and a number of LQ methods for working with oxides have been invented and perfected.

In the following are listed the main accomplishments of this ARO program. It will be apparent that a large number of ideas have originated from this research.

II. LQ DEVICES

Shock tube method: This technique has been commonly employed to form LQ specimens. The original device was constructed by P. Duwez some years ago and represents the simplest means of fabricating a porous and flaky specimen. With some care, a semi-continuous foil is formed, permitting SAXS studies. Generally, the TEM specimens do not have to be thinned, since a significant proportion of the foil is electron transparent and requires no further thinning. However, we have available an ion thinner and using this thinning technique enables us to obtain an extremely fine specimen for TEM, for both alloys and ceramic materials. .

Torsion Catapult: This method was developed in order to obtain a more continuous foil. A program was carried out using Al-base Ag, in which SAXS was employed to examine spinodal decomposition following torsion catapult LQ. In this method a molten specimen is propelled out of a curved furnace by the

released energy stored within a torsion catapult. The specimen then strikes a copper slide and rapidly solidifies (1).

LQ of Laser-Melted Oxides

Lasers offer attractive heat sources for LQ systems. We have in this program devised a new method for the LQ of oxides.

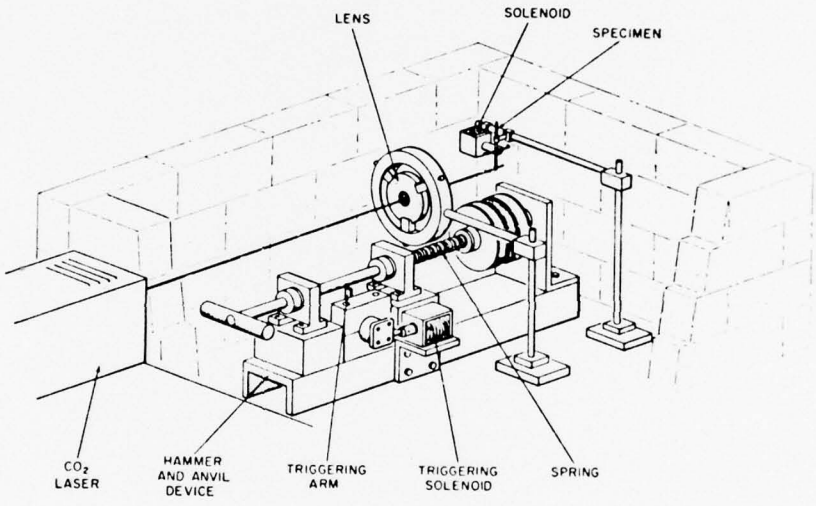

Figure 1

The technique utilizes a high intensity continuous-wave laser, together with a hammer-and-anvil quenching device (Fig. 1). The hammer-and-anvil apparatus is similar to that first developed by Pietrokowsky (2). A liquid drop is caught between the copper faces of a rapidly moving hammer and a stationary anvil. Quench rates of about 10^5 °C sec^{-1} have been reported for metals quenched in this manner. Oxide quench rates are, however, expected to be lower.

A continuous-wave CO_2 laser with a maximum output of 400 W is employed. The beam is focused by means of a water-cooled gallium arsenide lens having a focal length of 12.5 cm. The radiation incident on the specimens has a power density of about 5×10^3 W cm^{-2}, with the beam defocused so that the incident spot diameter is approximately equal to that of the specimen rods (0.1 in.). It is found that droplets do not fall off the specimen rods because of high surface tension. A solenoid is, therefore, employed to knock molten drops off the specimens. A signal from this solenoid is used to activate the trigger solenoid, releasing the spring-loaded hammer.

The first material investigated was α-Al_2O_3 (99.5% purity). The melting point of this material (2050°C) is low enough to allow easy melting, but sufficiently high to test the feasibility of the technique. Several phases of alumina are obtainable under various conditions. The phases present in liquid-quenched specimens might be expected to reflect the quench rate.

Specimens generally weighed about 100 mg, with diameters ranging from 0.5 to 1.5 in. and maximum thicknesses of approximately 0.002 in. (50 μm). Edge regions, however, were much thinner. The central regions of some specimens were almost transparent. Debye-Scherrer analysis revealed that these transparent central areas were composed largely of metastable δ-alumina. The outer edges of the specimens were predominantly α-alumina, which is the usual phase obtained when Al_2O_3 is solidified normally from the melt. The quench rate for the center of a specimen should indeed be higher than that for the outer edges, since the center makes contact with the hammer-and-anvil faces first.

Specimens suitable for TEM were prepared by means of ion-thinning. Selected-area diffraction indicated that δ-alumina is obtained at the center. Also, there is good evidence that an amorphous oxide layer is formed adjacent to the anvil faces.

III. REVIEWS OF ALLOY SYSTEMS STUDIED IN THIS PROGRAM

Al-7 Zn

The kinetics of GP zone formation in liquid-quenched Al-7at.% Zn was studied with small-angle x-ray scattering. It is found that liquid quenching yields a solid solution in the as-quenched condition which is significantly less clustered than for solid quenching. In addition, the aging kinetics of the liquid-quenched specimens was observed to be significantly slower than that for solid-quenched specimens. The results indicate that slow aging in liquid-quenched alloys results from the absence of a high concentration of quenched-in mobile vacancies. It is thus suggested that liquid quenching effectively enables studies of the earliest stages of phase separation in precipitation hardenable alloys.

Al-22 Zn

study was initiated on this alloy because Rundman and Hilliard con- that spinodal decomposition is occurring on aging at 65°C after SQ (3). However, an unexplained early transient led to some uncertainty as to the exact mode of decomposition. In fact, the main question was whether solute clustering, which might have occurred during the quench, would confuse the interpretation of the results (4). It is known that bulk Al-Zn has a strong tendency to decompose during quenching (5). We thus undertook to resolve this question by LQ of Al-22 Zn. LQ should result in a more random (i.e. supersaturated) solid solution.

Indeed, a particularly suitable application of LQ should be in studies of early-stage spinodal decomposition. When the free energy of a supersaturated solution can decrease with the development of the smallest fluctuation in composition, the solution is unstable and can decompose spontaneously. In this situation, the essential limitation to the formation of a new phase is

kinetic, since the only barrier to solute partitioning is diffusion. Thus, up-hill diffusion (the development of gradients) is possible in regions of the free energy-composition plot where the second derivative of the free energy relative to composition is negative; $\partial^2 f/\partial c^2 < 0$. Based upon this premise, a kinetic theory has been formulated which predicts that decomposition will occur by the selective growth of sinusoidal composition fluctuations (6). The fluctuations will have a narrow band of wavelengths clustered around one having a maximum growth rate. The occurrence of the maximum is due to a balance between two competing effects: (1) The growth rate increases with decreasing wavelength because of a reduction in diffusion distance; and (2) The gradient energy increases with increasingly sharper composition fluctuations, i.e. with decreasing wavelength. The wavelength for which the growth rate is the maximum will depend on temperature and solution parameters.

An approach particularly useful for studying the spinodal mode is due to Rundman and Hilliard, who recognized a formal correspondence between the Fourier amplitudes of the composition fluctuations and the amplitude of the x-rays scattered by these fluctuations (3). The x-ray intensity profile, and its development with time, is thus shown to be related to the evolving composition fluctuations. If the system is undergoing spinodal decomposition, and the composition gradients are not severe (i.e., early in the reaction), then the rate of growth of the fluctuations can be determined. Actually, it is the growth of the Fourier components which is being studied by this x-ray method. The kinetic parameter in question is $R(\beta)$, the amplification factor for a given Fourier component having a wavenumber β.

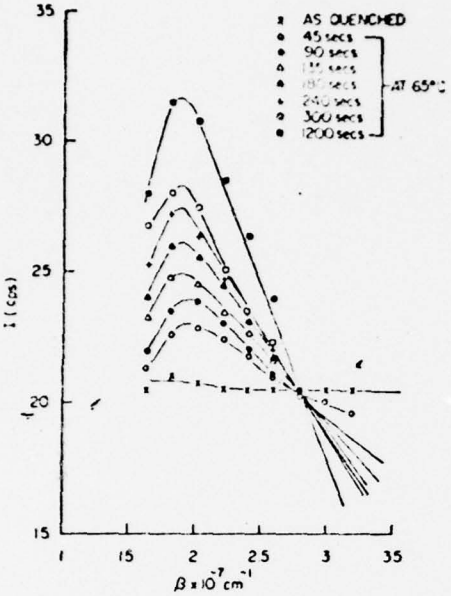

FIG. 2
The evolution of the intensity - wavenumber profile as a function of time for aging LQ Al-22 Zn at 65°C. (After Reference 7).

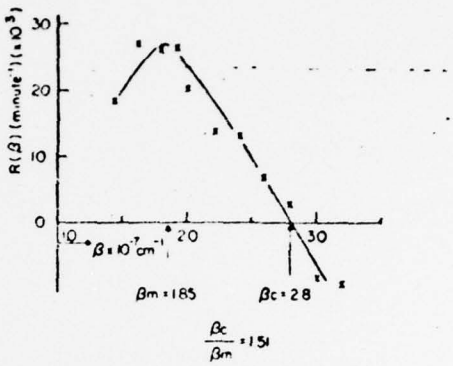

FIG. 3,
Amplification factor vs. wavenumber from the data of Fig. 2.

In Fig. 2 is shown the SAXS spectra for the as-LQ condition and for aging at 65°C for early times (7). In this plot, β is the wavenumber of the decomposition waves, and is equal to 2π times the reciprocal of the decomposition wavelength. The intensity at a given β can be considered to be directly related to the number of those waves having that β. Fig. 2 thus represents a kinetic view of the distribution of the evolving two-phase structure. One can immediately conclude that (i) the system is decomposing by the formation of waves having wavelengths grouped around 34A°; (ii) waves having wavelengths below a cross-over point of about 22A°'s are going into solution.

R(β) can be extracted from the data of Fig. 2. This is plotted in Fig. 3 and shows the rate of both growth ($\beta < \beta_c$) and decay ($\beta > \beta_c$) of the decomposition waves. This plot demonstrates that spinodal decomposition is in fact occurring here and that the process is being observed at a sufficiently early time so that the linear theory is applicable. The results

are very similar to those obtained by Rundman and Hilliard for SQ of the same alloy. LQ, on the other hand, removes the ambiguities which arise from solute clustering occurring during the quench. TEM studies give further support for a spinodal mode: A multiply-connected structure is observed having a spacing comparable to that observed with SAXS.

In our view, LQ is a perfectly appropriate way of obtaining a well-quenched supersaturated solid solution. Further experiments of this sort will be described for Al-Ag.

Al-28 Zn

In the composition range of 28% Zn are found various continuous transformation products as well as a grain boundary nucleated cellular product. The latter tends to dominate the reaction, absorbing the continuous product in its path. It was of some interest to study the decomposition of LQ Al-28 Zn in an effort to delineate the early products of decomposition.

SAXS has been used here to follow the early-stage process by examining the developing integrated x-ray intensity during the growth of the cells. A parameter, $Q \propto \int_0^\infty I(2\theta)^2 d\theta$, can be used as a measure of the relative volume fraction of a phase. In this expression, I is the intensity scattered to a diffraction angle, 2θ. When $I(2\theta)^2$ is plotted versus scattering angle, the distribution of scattered x-ray intensity can be related to the size of the particles. Also, particle spacing $= \lambda/(2\sin\theta) \tilde{-} \lambda/2\theta$ (for small angles) where λ is the x-ray wavelength. This reciprocal relation between spacing and scattering angle permits us to relate the scattered intensity to a given spacing. In Fig. 4 is plotted $I(2\theta)^2$ vs. 2θ for as-LQ, 35 minutes and 200 minutes at 65°C. The maximum that occurs at 10 millirads ($\sim$155A°) is due to the continuous matrix phase. The maximum decreases with time and eventually shifts to lower angles; i.e., the product phase undergoes coarsening. This higher angle peak represents the diminishing continuous phase. Having a

spacing initially of 400A°, the lower angle peak, at less than 4 millirads, is due to the cellular phase; its position does not change with time, but its intensity increases due to the growing cellular phase.

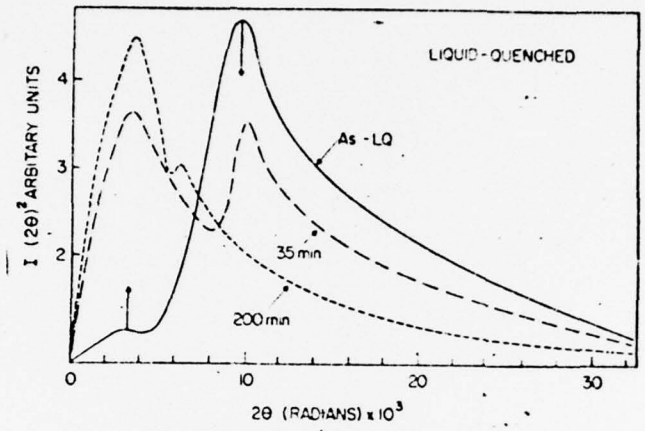

FIG. 4
$I(2\theta)^2$ vs. 2θ for aging of LQ Al-28 Zn at 65°C for different times. (After Reference 8).

Analyses of this sort, using both TEM and SAXS, lead to the following conclusions for the Al-28 Zn alloy (8):

1. The as-quenched state is characterized by a grain boundary discontinuous phase and some decomposition in the matrix for both the LQ as well as SQ specimens.
2. SAXS results indicate that LQ leads to a sharper particle size distribution than SQ for the continuous phase; in the as-quenched state and also during aging.

Al-Ag

The Al-base Ag system has been studied for many years and can be considered to be the prototype ideal G.P. zone-forming system. This system is attractive for several reasons: (i) It has been thought that there is little strain associated with the formation of zones; (ii) The zones are spherical, permitting polycrystalline specimens to be employed for SAXS studies; (iii)

There is a large difference in atomic scattering factor between Ag and Al, and therefore the scattered x-ray intensity is large at small angles. A good deal of study has thus gone into characterizing the kinetics, the metastable equilibrium limits and the metastable structures in this system.

On the other hand, detailed SAXS studies have not led to unambiguous results. And in fact, attempts to obtain a linear spinodal mode in this system have not been particularly successful.

LQ presents the possibility of obtaining Al-Ag in a very well quenched condition. It may then be possible to overcome the problems arising from quench-clustering. That this is in fact is possible has been shown by Roberge and Herman for Al-14 Ag (9). Spinodal decomposition of LQ Al-15 Ag was studied for aging at 150°C of both LQ and SQ specimens. Linear behavior was found for both of these specimens, with the LQ giving a predictably smaller decomposition wavelength than for SQ; 112A° vs. 125 A°. Also, consistent with what has been found in our studies of Al-base alloys, the SQ specimen decomposes more rapidly than does the LQ specimen; the R(β) at the maximum wavelength is twice as large for SQ. This we attribute to a lower concentration of mobile vacancies for the LQ condition than for the SQ condition.

These results represent a sampling of our results in spinodal decomposition in LQ-Al-base alloys, and, taken together with those for Al-Zn, point to the efficiency of LQ in obtaining a well-quenched solid solution.

The as-LQ condition was examined and indeed found to have a narrower size distribution than that obtained for SQ (9). SAXS was used to characterize the cluster size distribution for LQ and SQ Al-14 Ag.

TABLE 1

Radius in A° and Weight Fraction for LQ (Gun Technique) and SQ (550°C → Brine at -22°C) Al-14 Ag.

Condition	Radius (A°)	Weight Fraction
SQ	7.5	0.60
	21.0	0.25
	27.0	0.15
LQ	6.5	0.96
	15.0	0.04

In Table 1 is shown the radii and weight fractions as determined from size distribution of the radii of gyrations resulting from Guinier plots of SAXS profiles. It is seen that for LQ, the sizes are shifted to lower values and the size distribution is much narrower. This distribution then represents an improved starting point for decomposition studies.

These results indicating a less clustered solid solution for LQ than for SQ have been confirmed by lattice parameter measurements for Al-base alloys with Si and Ag (this program).

Al-Si

Precipitation in LQ Al-base Si has been studied. For SQ alloys it is well established that Si precipitates are nucleated heterogeneously on dislocation loops arising from the coagulation of excess quenched-in vacancies. It was thus of some interest to study the decomposition kinetics in LQ alloys. If there are available more vacancies in LQ, then the nucleation rate and, therefore, the kinetics of decomposition should be faster than for SQ. That this is not the case is seen in Fig. 5, where the percentage

change in electrical resistance is plotted versus time for aging LQ Al-1 wt.% Si at 200°C. For a comparable change in resistance (~4%), the SQ alloy takes about 60 minutes, whereas for LQ, several hundred minutes are required. It would appear that LQ results in fewer vacancies.

Precipitation in LQ Al-Si, however, does occur similarly to that in SQ alloys. TEM photos of LQ Al-1 wt.% Si show a general absence of dislocations. However, such defect-clear regions are not obtained uniformly throughout the specimens. Regions are observed where the dislocation density is high and numerous dislocation loops are seen. Such effects may result from non-uniform cooling rates and from plastic deformation, either during the ultra-rapid solidification process or, subsequently, during handling. Following aging for 50 minutes at 200°C a high, uniform density of fine Si particles form. These particles are similar in distribution and shape to those observed in SQ studies. Also, since the kinetics, as depicted in Fig. 5, is similar for both SQ and LQ, it must be concluded that only the particle density for the two differ, the LQ giving a lower density. This is not easily confirmed by TEM because of the non-uniform thickness of the LQ foils. And, indeed it is this problem which has limited careful TEM work with LQ specimens.

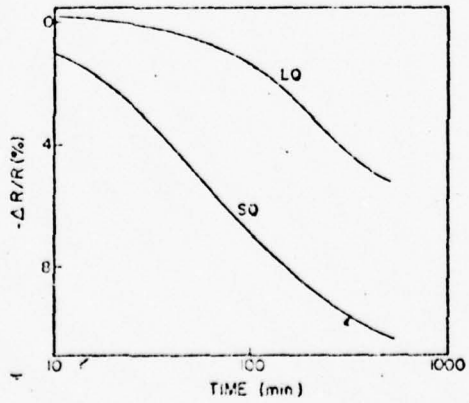

FIG. 5
Isothermal aging at 200°C of LQ and SQ Al-1 wt.% Si.

Ag-Ge

The formation and decomposition behavior of metastable structures in liquid-quenched (LQ) Ag-Ge alloys was studied with x-ray diffraction, resistivity measurements and TEM techniques. Pure Ag and alloys containing 7,10,15,20 and 22.5 at.% Ge were studied. Upon LQ, pure Ag and 7 and 10 Ge alloys yield a single fcc phase; 15 and 20 Ge alloys give a mixture of two metastable phases (fcc and hcp); and the Ag-22.5 Ge alloy gives a metastable hcp phase. Also, the first evidence of an amorphous phase in as-LQ Ag-22.5 Ge alloy is presented. It is shown that Ag-rich fcc phase can retain up to ∿20 at.% Ge in solid solution. Furthermore, stacking faults play an important role in the formation and decomposition of metastable phases in the Ag-Ge system.

Au-Ge

The decomposition behavior of various metastable phases obtained by liquid quenching of eutectic Au-27 at.% Ge was studied by electrical resistivity measurements, x-ray diffraction and TEM techniques. The as-liquid-quenched structure is found to consist mainly of equilibrium Au-rich fcc α-phase and metastable bct γ-phase. In addition, the equilibrium Ge-phase and another metastable phase hcp-β are also found to be present as minor constituents. Upon heating, phase decomposition occurs in two distinct stages: A low temperature stage, 60°-100°, involving the decomposition of the β-phase into two equilibrium phases, Au-rich fcc-α and Ge. A second stage, occurring around 120°C, consists of the transformation of the γ-phase into α and Ge.

IV. OXIDES WHICH HAVE BEEN STUDIED

In the following will be outlined those experiments carried out on pure and mixed oxide systems with laser and plasma techniques.

A. Laser Hammer-and-Anvil

Successful oxide splat-quenching, using α-alumina as a starting material, was achieved utilizing a CO_2 laser in conjunction with the hammer-and-anvil quenching device. Specimens were generally 50-70 μ thick and weighed ∿50-100 mg. Debye-Scherrer analysis revealed a phase distribution consisting of stable α-alumina at outer specimen regions and δ-alumina (metastable) in central regions, where the quench rate was the highest. Some evidence suggests the presence of other metastable phases. Electron diffraction work has supported the above results. TEM observations of the as-quenched microstructure has revealed the very fine equiaxed grain structure typical of hammer-and-anvil quenched specimens.

The first mixed oxide system investigated has been Al_2O_3-MgO. So far, alloys of ∿39 and 29 mole % MgO have been successfully quenched. D.S. analysis has revealed the presence of the spinel phase only. TEM investigation of the as-quenched material has revealed largely featureless grains. Some apparently amorphous material has been detected. This may be a manifestation of the splat surface only, and ion thinning from one side only to preserve surface structure were in general performed for all as-quenched specimens. Annealing studies were carried out to investigate the modes of phase decomposition. Additional specimens prepared for splatting included ∿10 mole% MgO, ∿18 mole% MgO single xtal, and MgO rich compositions.

ZrO_2-30 mole% CaO has also been successfully quenched. Although specimen surfaces were extremely glossy and varied in color from white to brown, x-ray analysis revealed only equilibrium phases.

Other specimens prepared for quenching include Al_2O_3-10 mole% Y_2O_3, which should yield quench rate information by means of eutectic interlamillar spacing measurement, and Al_2O_3-30 wt.% CaO, which has been partially transformed to

glass by laser melting and air quenching.

B. Laser LQ (Gun Blast)

Laser LQ was performed on several unary and binary systems to obtain metastable and perhaps glassy phases and further document transformation reactions. The samples were pressed, presintered at 1500°C in a Kanthal high temperature furnace, and melted in air with a CO_2 laser. A gas-type LQ gun with a platinum nozzle was used to impinge the sample onto a copper ski slope. In certain mixed oxide systems carbonate powders were found to produce better sintered oxide products for quenching. The LQ systems are:

1. Unary Systems

   $MgAl_2O_4$ (stoichiometric)

   $SrTiO_3$

   $MgTiO_3$

   $CaTiO_3$

   $BaTiO_3$

   TiO_2

   CoO

   GeO_2

   Al_2O_3

   $CoTiO_3$

2. Binary Systems

   $BaTio_3$ - $CaTiO_3$*

   NiO - CaO*

   Al_2O_3 - SiO_2

   CoO - NiO*

   CoO - MgO*

   MgO - $MgAl_2O_4$

   $MgAl_2O_4$ - Al_2O_3

CaO - MgO

TiO_2 - SnO_2*

*Note these systems unsuccessfully LQ by regular gas-type gun and induction heating.

C. Theoretical calculation of the coherent spinodal in ionic and metallic cubic binary systems and comparison with experimental data (see attached diagrams and tables). Systems predicted using technique outlined in the Thesis of C. Jantzen (in preparation):

CoO - CaO

CaO - NiO

CoO - NiO

CaO - MgO

MgO - $MgAl_2O_4$

$MgAl_2O_4$ - Al_2O_3

AgCl - NaCl

KCl - NaCl

Al - Zn

Au - Pt

Au - Ni

D. Redetermination of the metastable miscibility gap and confirmation of spinodal decomposition in roller quenched Al_2O_3 - SiO_2 glasses by SANS and electron microprobe.

E. Solid quench and pertinent TEM of CoO - NiO. Aging in heating holder of electron microscope produced reduction of CoO to metallic cobalt.

F. Studies of phase transformations in $MgAl_2O_4$ - Al_2O_3 ($MgO \cdot 3Al_2O_3$) by SANS and x-ray diffraction.

V. PLASMA SPRAYING OF OXIDES

A. Introduction

Protective plasma-sprayed ceramic coatings, although extensively studied from the engineering viewpoint, have received limited microstructural analysis. However, the unique processes inherent in plasma spraying are known to produce structures which are vastly different from the equilibrium structures obtained by other processes. For example, metastable phases are found in plasma sprayed Al_2O_3 and their reversion to the equilibrium phase can produce internal stresses and failure of the coating. An understanding of the microstructure and phases present in a coating and the influence of subsequent annealing, alloying additions, etc. would be invaluable in predicting the behavior of a coating in service. With this aim in view a study of the macro-, micro- and crystal structures of sprayed ceramic deposits has been made by scanning electron microscopy (SEM), transmission electron microscopy (TEM) and x-ray diffraction.

The porous "pancake" morphology, generally produced by plasma spraying, results from the rapid flattening of superheated liquid particles impinging, essentially independently, on the substrate or previously deposited layer. Since the flattened particles are usually well bonded together, the main concern for the integrity of the coating system is the coating/substrate adhesion. Thus, in this study emphasis has been placed on a detailed analysis of the structure and morphology of the ceramic at the interface.

B. Sample Preparation

Plasma sprayed samples of Al_2O_3, Al_2O_3-Y_2O_3, Al_2O_3-MgO, ZrO_2, Al-1.6% Si (Table 2) have been prepared as described below. Except where specific differences in structure occur, only the results of Al_2O_3 deposits will be presented since they are, in general, typical of the ceramics examined.

Ceramic deposits of thickness ranging from 25 to 750 μm were sprayed on onto grit blasted mild steel substrates by a hand-held torch, energized by a 28 KW spray system using the parameters given in Table 3. The samples were characterized in both the as-sprayed and annealed conditions. Annealing treatments were carried out in an argon atmosphere at temperatures ranging from 600°-1200°C.

Thin foil samples were subsequently prepared by ion-thinning. This process involves bombarding the surface of a small (∿3 μm dia. X ∿20-30 μm thick) section of the material with argon ions thereby removing atoms from the sample surface. Schematic diagrams of the working chamber and sample holder are shown in Fig. 6. The thinning parameters used for the current samples are given in Table 4.

The ion thinning technique has several advantages over the more commonly used electrochemical methods, particularly for the relatively inert ceramic materials. Material removal is more uniform and thus preferential etching, for example at grain boundaries or second phases is essentially eliminated. For the study of interfaces, the technique has the particular advantage of making it possible to remove metal substrate and ceramic coating at approximately the same rate. The electrochemical dissolution, on the other hand, would inevitably result in more rapid removal of the metal, making examination of the interfacial layers of the substrate impossible.

In an attempt to gain a better understanding of (i) the mechanisms involved in coating/substrate adhesion, (ii) the effects of a change in cooling rate on the microstructure and (iii) the nature of the coating itself, sections perpendicular to the interface were cut. These were then thinned as described above. For both TEM and SEM, samples were coated with a ∿200A° thick layer of carbon or gold, respectively, to prevent charging of the insulating ceramic by the electron beam.

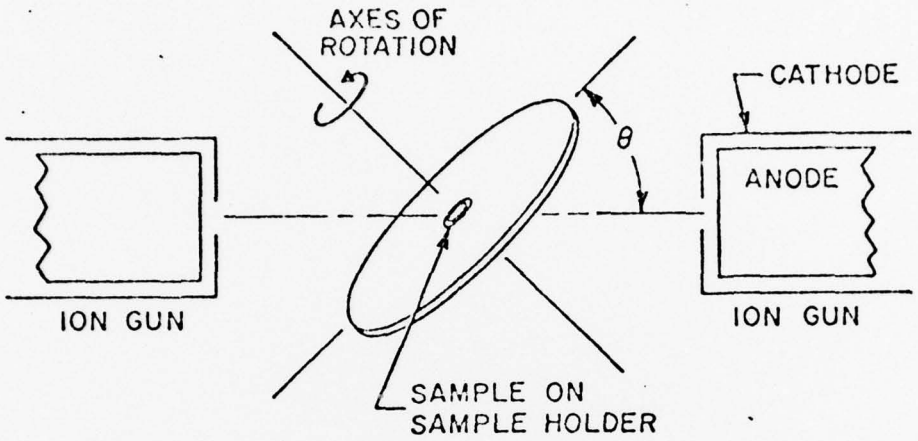

(a)

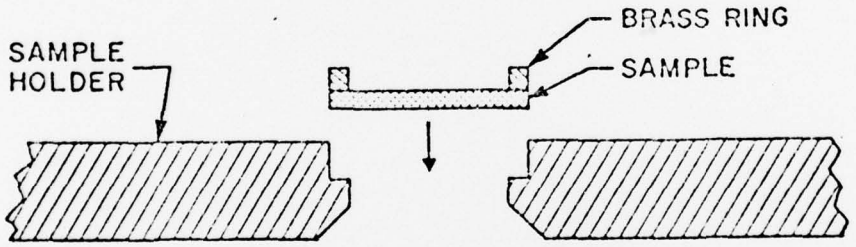

(b)

Fig. 6 Schematic of the geometry of the ion-thinning chamber demonstrating the relative positions of the sample and the ion beam (a), and an enlarged view of the sample mounting configuration (b).

C. Characterization of Coatings

X-Ray analysis of the various samples was performed on Siemens X-Ray equipment with a Debye-Scherrer camera and a diffractometer which was used in conjunction with a carbon single crystal monochromator. Electron microscopy was performed using a Cambridge Mark II Stereoscan and a Philips EM300 microscope.

RESULTS AND DISCUSSION

Splat Cooled Nature of Plasma Sprayed Deposits

Due to the fact that the superheated particles are ejected with the order of sonic velocity and impinge on a highly conductive surface, the solidification process is extremely rapid. In fact.solidification rates on the order of 10^6 to 10^8 °C/sec. for metals, and 10^4 to 10^6 °C/sec. for oxides are obtained. The solidification rate for plasma sprayed Al-1.6 $^{w}/_{o}$ Si (sprayed onto a low conductive glass substrate) is estimated to be 10^6 °C/sec. This rate was obtained utilizing an equation for the determination at splat-cooling rates based on the scale of microstructure. The dendrite spacing in Figure 7 is used to approximate the solidification rate, which shows two SEM's of Al-1.6 $^{w}/_{o}$ Si plasma sprayed onto a glass substrate in a single pass.

As a consequence of the rapid cooling rates, plasma spraying may be considered to be splat-cooling and, therefore the microstructures of the materials obtained from both processes should be similar. Comparative structures of ceramics produced by splat cooling and plasma spraying are not available, but the transmission electron micrographs of Al-Si alloys shown in Fig. 8 illustrate the similarity. Fig. 8a shows the alloy splat-cooled by the Duwez gun technique and Fig. 3b by plasma spraying. Both micrographs exhibit fine, columnar grain structures within each platelet, $\sim$0.5-1.0 μm in width and $\geq$ 3 μm long. A similar structure is also obtained for Al_2O_3

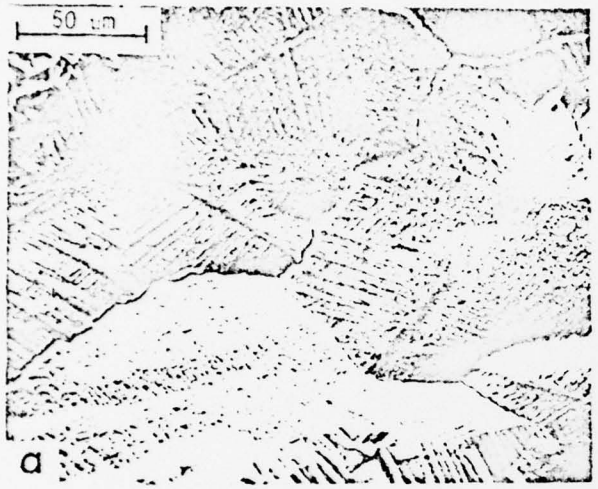

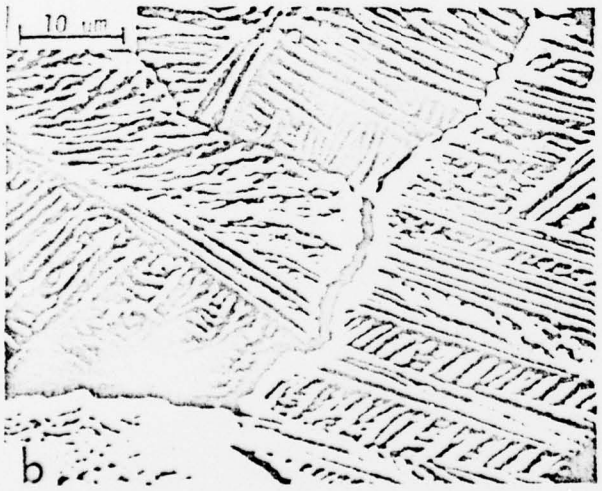

Fig. 7 Scanning electron micrographs of Al-1.6W/o Si sprayed on a glass substrate. Figure b shows an enlarged view of the central region in a.

Fig. 8 Comparison of transmission electron micrographs of Al-1.6W/o Si as splat-cooled [15] (a) and plasma sprayed (b); and Al_2O_3 plasma sprayed (c).

(Fig. 8c).

The morphology of the coatings was examined by SEM which, because of its high resolution and depth of field, enabled the overall lamellar nature of the coating and the grain structure of the individual platelets to be observed in detail. Figure 9 shows these features in an Al_2O_3 sample which was sprayed at 90° to the substrate. Coatings sprayed at angles less than 90° have more asymmetric morphology with lower coherency between the particles.

A process-inherent temperature gradient is produced throughout the substrate and coating which creates residual stresses and, consequently, results in microcracking in brittle materials such as Al_2O_3. Furthermore, because of the rapid quenching many particles partially solidify before a uniform flow is achieved. Thus, they are unable to fill all cavities in the previous layer and the resulting structure has a porosity of $\leq$ 12% (10). Both pores and microcracks are precursors to failure and should in general be avoided.

The columnar grain structure within the platelets is typical of the pure ceramics. However, additions of other oxides, eg. Y_2O_3 or TiO_2, results in a more equiaxed grain morphology, Fig. 10.

A number of metastable, high temperature phases are observed in thermally sprayed Al_2O_3, instead of the stable α (corundum). Such phases have been reported earlier (11-13) but, in the present investigation, a dependence of the specific polymorphs of alumina on the cooling rate of the deposit has been detected. In plasma sprayed Al_2O_3, the common high temperature phases are δ, θ with some γ and α, whereas in the low temperature oxyacetylene spray process the common phase is γ, with some θ and α. In very thick plasma sprayed coating (>250 μm) very little δ and θ have been observed, here the predominant phases being γ and α. Thus, it appears that thicker coatings

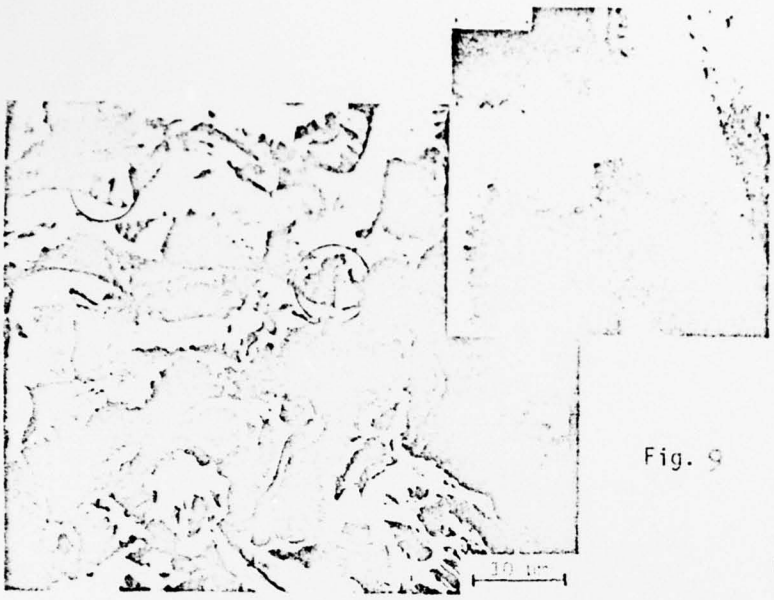

Fig. 9 Scanning electron micrograph of a typical Al_2O_3 plasma sprayed coating cross-section, showing the columnar structure. In comparison a transmission electron micrograph of such a grain structure is shown in the inset.

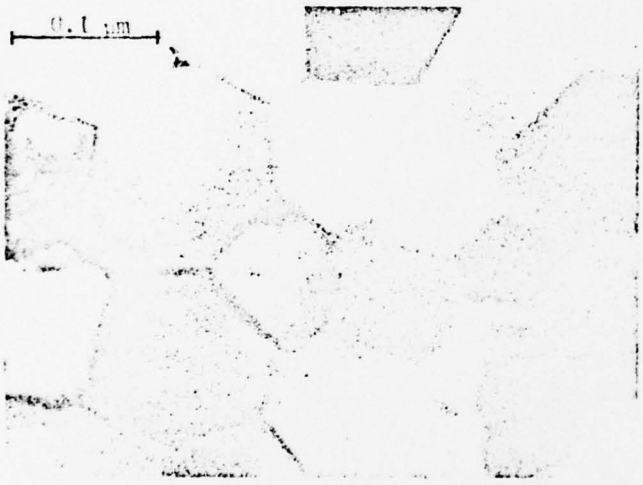

Fig. 10 Transmission electron micrograph of plasma sprayed Al_2O_3-Y_2O_3, showing the typical equiaxed grain structure caused by additions of the Y_2O_3.

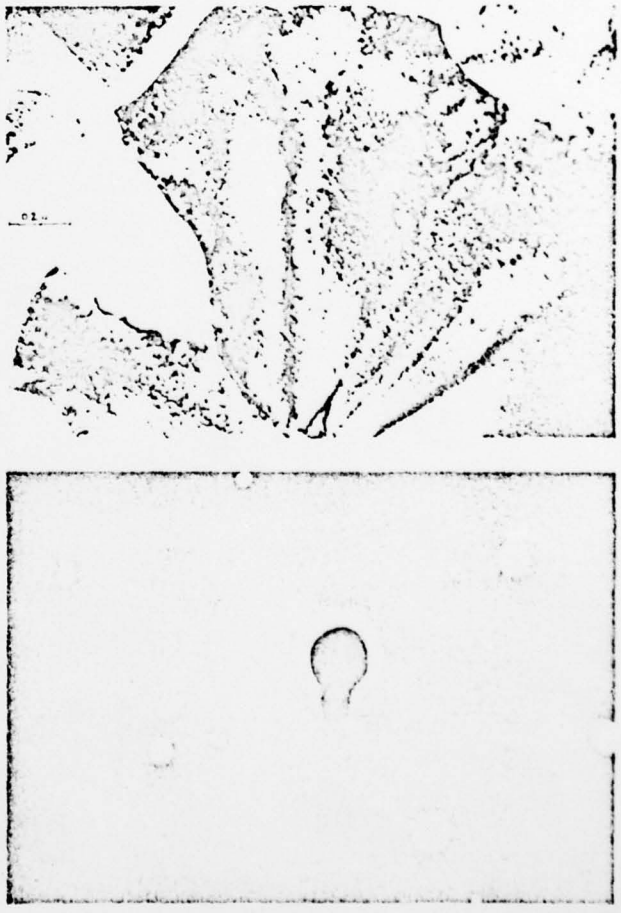

Fig. 11 Transmission electron micrograph of plasma-sprayed Al_2O_3 with the corresponding selected area electron diffraction (SAD) pattern of the center grain.

are cooled more slowly because of the poor conductivity of a ceramic coating and the repeated reheating of the gun as it is passed over the work piece. This process anneals the layers of the coating already deposited enabling the structure to equilibriate to the stable corundum phase. These observations show that a thick plasma-sprayed coating will be more similar to the lower temperature flame spray process, at least from the point of view of metastable polymorphs.

Samples annealed at 1000°C for 1 hour or more underwent definite structural change as indicated by x-ray diffraction line broadening and shifting. Moreover, some diffraction peaks disappeared and others began to emerge. The former corresponded to either γ or δ-Al_2O_3 and the emerging peaks were all those of the α-phase. For samples left a 1100°C for 2 or more hours, the reversion to corundum was almost complete. Associated with a crystal structure change is a lattice parameter change and, consequently, a volume change. With the reversion from the metastable structures in Al_2O_3 to corundum there is a shrinkage associated, which in the case of the reversion from $\delta \rightarrow \alpha$ is $\sim$8%. This leads to microcracking of the deposit and possible coating failure.

Selected area diffraction (SAD) of ion-thinned samples of the sprayed ceramics confirmed the presence of the metastable polymorphs. Fig. 11 shows a grain of Al_2O_3 and its corresponding electron diffraction pattern. The major spots are indexed as δ-Al_2O_3, whereas the streaked spots are indexed as the next lower temperature polymorph, θ-Al_2O_3. The streaking is caused by a particle size effect. The emergence of the θ-phase may have occurred during the solidification process or may be due to local beam heating in the microscope. The sequence of emerging Al_2O_3 phases observed with TEM is as follows:

$$\delta \rightarrow \theta \rightarrow \gamma \rightarrow \alpha$$

This sequence is consistent with the x-ray results of Dragoo and Diamond (14).

As discussed above and as shown in Fig. 8 there is a definite similarity between plasma-sprayed and splat-cooled metals. This similarity also holds for sprayed ceramics as was shown in Fig. 8. In plasma sprayed coatings the grain shapes vary, beginning with grains elongated several micrometers in the plane of the platelet for the first several layers and perpendicular for later ones. This phenomena is due to the liquid spreading outwards from areas where solidification has initiated. In thicker sections, i.e. farther into the coating, we find columnar growth normal to the substrate surface. This is a characteristic structure in ingot solidification. Furthermore, it is interesting to note, that columnar growth normal to the deposition surface or parallel to the direction of heat flow is also reported in sputter-deposited films (15).

An observed amorphous interface layer may have the effect of enhancing the bond strength of the coating to the substrate. It is suggested that at the time of impingement the Al_2O_3 is a highly viscous liquid, a glassy amorphous material, and thus attains better mechanical contact with the substrate. Furthermore, it appears probable that the molten alumina dissolves the initially formed iron oxide of the steel substrate and may go into solution and form an aluminum-iron spinel.

The columnar-type fine grained structure observed by SEM correlates with the TEM observations (shown in an inset in Fig. 9) and is characteristic of sprayed coatings. However, if impurities such as Y_2O_3 (3%) are added to Al_2O_3 the grains become equiaxed, although the columnar macrostructure is maintained. This may be due to grain boundary pinning caused by Y_2O_3 or other "fluxing" materials.

There are other important aspects of these additives. For example, Y_2O_3 acts as a glass former and not only decreases the porosity of the coating but also enhances the adhesion (10). These beneficial effects of Y_2O_3 (3% to 10%) are attributed to the flass forming ability of the second phase which solidifies at a temperature well below the solidification temperature of Al_2O_3 (2060°C). It is, therefore, able to flow more readily enabling a more complete interaction with the sandblasted substrate surface. This causes an infilling of the interstices between the platelets of the more rigid crystalline oxide.

In some cases additives will have a stabilizing effect on the sprayed materials. Thus, they will inhibit the formation of metastable phases. Furthermore, "fluxing" additions can retard or stop the reversion process of the metastable phases to the equilibrium structure. Since metastable structures are inherent to the rapid cooling rates obtained in sprayed coatings, there is a definite dependence of cooling rate and polymorph formation. Thus, in thick coatings or coatings deposited by lower temperature processes the occurrance is diminished. The difference between the specific volume of these phases and that of the equilibrium structure renders the susceptibility to cracking and spalling if a phase transformation occurs. This may easily be the case if the coating is exposed to a high temperature environment, and thus catastrophic failure may result. It may, therefore, be advisable that a crystallographic and microstructural study be made of any coating material that has known stable or metastable polymorphs, before the coating material is used.

TABLE 2

Coating Materials

Material	Purity (%)	Source
Al_2O_3	99.28	Norton #183
Al_2O_3	99.+	Cerac #1004
Y_2O_3	99.9	Ventron
$MgAl_2O_4$	99.+	Cerac #1117
ZrO_2 (stabilized)	94.4	Norton #252
Al-1.6w/o Si	99.99	Alcoa (wire)

TABLE 3

Spray Parameters (Ceramic Powders)

Arc current	400a
Arc voltage	48v
Arc gas	
argon (primary)	241 x 10^{-2} m^3/hr[a]
hydrogen (secondary)	14.2 x 10^{-2} m^3/hr[a]
Powder feed rate	7.0 gm/min
Powder carrier gas	
argon	10.8 x 10^2 m^3/hr[a]
Gun to substrate distance	7.5 to 12.5 cm

[a] Gas pressures 3.45 x 10^5 Pa

TABLE 4

Ion-Thinning Parameters (Ceramics)

Acceleration potential	5-6 kV
Gun current	<0.5 ma
Ion current	75-100 μa
Glanzing angle (θ)	15°-25°
Sample thickness (initial)	25-35 μm
Thinning time	
initial @ 25° (θ)	3 hours
total	12-17 hours

VI. CONCLUSIONS

The central thrust of this ARO-supported research program has been the establishment of metastable structures through the use of liquid quenching methods. We have employed a wide range of techniques to rapidly quench liquid alloys and refractory oxides. A great deal has been learned about the earliest regime of the precipitation processes which these unique materials are observed to undergo. It has been possible to find a spinodal mode in LQ Al-22 Zn and in LQ Au-Pt alloy. The more detailed questions as to whether or not the mode is truly of a linear sort or otherwise, we feel, is resolved in Al-22 Zn, but, this unfortunately is not readily seen in the other alloys which were studied.

The vacancy concentration, at least those that are mobile, is seen to be low and does not contribute to rapid decomposition kinetics. High vacancy concentrations are not detected in As-LQ alloys due to loss during or immediately following LQ at the surfaces and at the very closely located

grain boundaries. Another effect, as yet unclear, is the possibility that the vacancies are not brought into the solid after the passage of the rapidly moving solid-liquid interface. More work is needed to resolve this question.

The laser and plasma spray techniques have been used to study the structure of as-LQ oxides and subsequent precipitation behavior. Here, spinodal decomposition was sought in, for example, the system Al_2O_3-SiO_2, which is amorphous when LQ. SANS studies at ILL-Grenoble, France, as part of this study, again point to the operation of a spinodal mode. But, here the situation is far more complex than it is for the alloy systems which we have studied.

Plasma spraying is an underutilized and certainly insufficiently appreciated technique for forming metastable alloys and oxides (not to mention carbides and composites). We have examined microstructure, kinetics and properties of oxide coatings formed by plasma spraying. Two problems remain: excessive porosity and, sometimes, poor coating-substrate adhesion. These limitations, we feel, however, can be avoided by atmosphere-control and vacuum spraying. Here, velocities of the spray increase and, for metals, oxidation is minimized, or essentially avoided.

REFERENCES

1. R. Roberge and H. Herman, J. Materials Science,
2. P. Pietrokowsky, Rev. Sci. Inst. 34 (1963) 445.
3. K. B. Rundman and J. E. Hilliard, Acta Met., 15 (1967) 1025.
4. G. Gerold and W. Merz, Scripta Met. 1 (1967) 33.
5. E. L. Huston, J. W. Cahn and J. E. Hilliard, Acta Met. 14 (1966) 1053.
6. J. H. Hilliard, Phase Transformations, ASM, ch. 12, p. 497, (1970).
7. S. Agarwal and H. Herman, Scripta Met., 7 (1973) 503.
8. S. Agarwal, M. J. Koczak and H. Herman, Scripta Met., 7 (1973) 401.
9. R. Roberge and H. Herman, J. Materials Science
10. V. Wilms and H. Herman, "Plasma Spraying of Al_2O_3 and Al_2O_3-Y_2O_3", 3rd Inter. Conf. on Bulk Coatings and Thin Films, San Francisco, April 5-9, 1976.
11. N. N. Ault, J. Amer. Cer. Soc., 40 (1957) 69.
12. H. Meyer, Werkstoff u. Korr., 11 (1960) 601.
13. F. Eichorn et al, Netalloberft., 26 (1972) 212.
14. A. L. Dragoo and J. J. Diamond, J. Amer. Cer. Soc., 50 (1967) 568.
15. S. D. Dahlgreen and M. D. Merz, Met. Trans., 2 (1971) 1753.

VII. PUBLICATIONS RESULTING FROM THIS ARO-SUPPORTED PROGRAM

1. "Laser Alignment of X-Ray Small-Angle Scattering Cameras", M. J. Koczak and H. Herman, Review of Scientific Instruments, 41, 1907 (1970).
2. "Precipitation in Al-Base Ag Alloys Quenched from the Liquid State", R. Roberge and H. Herman, Fizika, 2 Suppl. 2, 6.1 (1970).
3. "Comments on Separation of Phases by Spinodal Decomposition in the Systems Al_2O_3-Cr_2O_3 and Al_2O_3-Cr_2O_3-Fe_2O_3", H. Herman and R. K. MacCrone, J. American Ceramic Society, 55, 50 (1972).
4. "Precipitation in Liquid-Quenched Al-Base Si Alloys", S. Agarwal, M. J. Koczak and H. Herman, Scripta Metallurgica, 7, 365 (1973).
5. "Phase Decomposition of Liquid-Quenched Al-28 at.% Zn", S. Agarwal and H. Herman, Scripta Metallurgica, 7, 401 (1973).
6. "Spinodal Decomposition in Liquid-Quenched Al-22 at.% Zn", S. Agarwal and H. Herman, Scripta Metallurgica, 7, 503 (1973).
7. "Precipitation in Liquid-Quenched Al-Base Ag", R. Roberge and H. Herman, J. of Materials Science (G.B.), 8, 1482 (1973).
8. "Phase Decomposition in Al-Base Alloys Quenched from the Liquid-State", S. Agarwal and H. Herman, Phase Transitions - 1973, Ed. L. E. Cross, p. 207, Pergamon Press, 1973.
9. "On the Microstructure of Liquid-Quenched Monotectoid Al-Zn", R. Roberge and H. Herman, J. of Metals (GB), 101, 339 (1973).
10. "On the Question of Spinodal Decomposition in Alkali Halide Mixed Crystals", C. Jantzen and H. Herman, J. Physics, D, GB, Applied Physics, 7, L45 (1974).
11. "X-Ray Diffraction Studies of Alloys Quenched from the Liquid State", S. C. Agarwal and H. Herman, Siemen's Review XLI (1974), p. 34.

12. "Phase Decomposition of Liquid-Quenched Al-14 at.% Ag - Small-Angle X-Ray Scattering Study", R. Roberge and H. Herman, J. Materials Science (G.B.) 9, 1123 (1974).

13. "Liquid Quenching of Laser-Melted Oxides", R. Krepski, K. Swyler, H. R. Carleton and H. Herman, J. Materials Science (G.B.), 10, 1452 (1975).

14. "Crystallography and Microstructure of Equilibrium and Metastable Phases Resulting from Plasma Spraying of Ceramics", V. Wilms and H. Herman, Proceedings of the 8th International Thermal Spraying Conference", 1976, p. 236, Amer. Welding Society, Miami.

15. "Plasma Spraying of Al_2O_3 and Al_2O_3-Y_2O_3, V. Wilms and H. Herman, Thin Solid Films, 39, 251 (1976).

16. "Neutron Small-Angle Scattering Study of Spinodal Decomposition in Al_2O_3-SiO_2 Glasses", C. M. Jantzen, D. Schwahn, W. Schmatz and H. Herman, Verhandl DPG (VI), 11 (1976) 594.

17. "Spinodal Decomposition - Phase Diagram Representation and Occurrence", C. M. Jantzen and H. Herman, PHASE DIAGRAMS - 1977; ed. A. M. Alper, Academic Press, Inc.

18. "Microstructural Investigation of Plasma-Sprayed Aluminum Coatings" S. Safai and H. Herman, International Conference on Metallurgical Coatings, San Francisco, April, 1977, Thin Solid Films, to be published.

19. "Phase Decomposition in Liquid-Quenched Eutectic Au-Ge Alloy", S. C. Agarwal and H. Herman, J. Materials Science, 1977; to be published.

20. "Liquid-Quenched Ag-Ge Alloys - An X-Ray and Metallographic Study", S. C. Agarwal and H. Herman, J. Materials Science, 1977; to be published.

21. "Early-Stage Phase Separation in Liquid-Quenched Al-7 at.% Zn", S. C. Agarwal and H. Herman, J. Materials Science and Engineering, 1977; to be published.